



Sopok Extra

**AIAA 97-2850**

**Thermochemical Erosion Modeling Of The 25mm  
M242/M791 Gun System**

Samuel Sopok, Peter O'Hara, George Pflegl  
Us Army Benet Laboratories,  
Watervliet, New York 12189

Stuart Dunn, Douglas Coats  
Software And Engineering Associates, Inc.,  
Carson City, Nevada 89701

**DISTRIBUTION STATEMENT A**  
Approved for Public Release  
Distribution Unlimited

**20040218 243**

**33rd AIAA/ASME/SAE/ASEE Joint Propulsion  
Conference & Exhibit**

**July 6 - 9, 1997 / Seattle, WA**

## THERMOCHEMICAL EROSION MODELING OF THE 25MM M242/M791 GUN SYSTEM

Samuel Sopok, Peter O'Hara, George Pfligl  
US Army Benet Laboratories,  
Watervliet, New York 12189

Stuart Dunn, Douglas Coats  
Software and Engineering Associates, Inc.,  
Carson City, Nevada 89701

### ABSTRACT

The MACE gun barrel thermochemical erosion modeling code addresses wall degradations due to transformations, chemical reactions, and cracking coupled with pure mechanical erosion for the 25mm M242/M791 gun system. This predictive tool provides gun system design information that is otherwise impractical. The nitrided A723 and 0.002" plated Cr/A723 wall materials are evaluated for erosion using the M242 Cycle A firing scenario. This complex computer analysis is based on rigorously evaluated scientific theory that has been validated in the rocket community over the last forty years. This gun erosion analysis includes the standard interior ballistics gun code (XNOVAKTC), the standard nonideal gas-wall thermochemical rocket code modified for guns (CCET), the standard mass addition boundary layer rocket code modified for guns (MABL), and the standard wall material ablation conduction erosion rocket code modified for guns (MACE). This analysis provides wall material erosion predictions and comparisons (ablation, conduction, and erosion profiles) as a function of time, travel (customer selected 6", 12", 30"), and number of rounds to barrel condemnation. These M242/M791 gun system predictions agree well with the standard wall heat transfer/temperature profile code (FDHEAT) and actual measured gun system erosion data.

### INTRODUCTION

The study of chemical reactions in flow systems (aerothermochemistry) was first described by von Karman in 1951<sup>1</sup>. The modification of the heat transfer coefficient (blocking) for the mass addition of chemically reacting wall material into the boundary layer was first described by Reshotko and Cohen in 1955<sup>2,3</sup>. The thermochemical erosion of reentry vehicle heat shield material for various chemically reacting systems was first studied by Denison and

Dooley in 1957<sup>4</sup>. This thermochemical erosion theory was unified/summarized by Lees (CalTech, TRW) in 1958<sup>5</sup>. The near exclusive use of Lees' now JANNAF standardized model<sup>6-8</sup> has stood the test of time and demonstrates that the major assumptions are still reasonable and valid.

Gun barrel technology has focused on reducing mechanical/metallurgical gun barrel failures with great success while gun barrel gas-wall thermochemical/thermal ablation coupled with aerodynamic flow erosion has intensified due to performance requirements demanding the use of high flame temperature propellants. Practical gun barrel design should address thermochemical and thermal ablation although the latter constitutes a poor design since the proximity of the wall solidus temperature should be avoided.

In 1992, after an exhaustive search, US Army Benet Labs teamed with Software & Engineering Associates (SEA) to successfully modify the JANNAF standard rocket erosion codes (TDK/MACE)<sup>6-9</sup> into the first comprehensive gun barrel thermochemical erosion modeling code that addresses wall degradations due to thermal (transformations), thermochemical (reactions), and thermomechanical (cracking) effects coupled with pure mechanical erosion (high speed flow, wear). SEA is the sole maintainer and developer of these rocket erosion codes. The CCET thermochemistry code is similar but much more robust than the BLAKE code<sup>10</sup>. The gun erosion analysis uses standard interior ballistics gun code (XNOVAKTC)<sup>11</sup> core flow data as input. In 1993, a joint SEA/Benet gun erosion workshop was held to introduce this code to the gun community<sup>9</sup>. Many ADPA Tri-Service sponsored gun erosion meetings have implied a thermochemical erosion mechanism for various gun systems including the M242/M791 gun system<sup>12-13</sup>. US Army experimental data supports the existence of gun barrel oxidation<sup>14</sup>. In July 1995,

Benet Labs and SEA jointly published (AIAA) the first known comprehensive gun barrel thermochemical erosion modeling code <sup>15</sup>.

### THEORY AND PROCEDURE

This paper models the 25mm M242/M791 gun system with its HC-33 propellant and 3200 K flame temperature <sup>12</sup>. This M242/M791 gun system <sup>12</sup> erosion analysis includes the standard interior ballistics gun code (XNOVAKTC for core flow) <sup>11</sup>, the standard nonideal gas-wall thermochemical rocket code modified for guns (CCET for g-w transport/chemistry) <sup>6,8,9</sup>, the standard heat transfer modified by mass addition to boundary layer rocket code modified for guns (MABL for transport & cold/adiabatic wall properties) <sup>6,9</sup>, and the standard wall material ablation conduction erosion rocket code modified for guns (MACE) <sup>7,9</sup>. The XNOVAKTC code and its core flow output is well known to the gun community and the reference is recommended for more information <sup>11</sup>.

The CCET code <sup>6,8,9</sup> outputs gun system inert/reacting G-W enthalpy ( $H_{gw}$ ), condensed phase products mass fraction ( $C_{cg}$ ), and ablation potential ( $B_a$ ) data as a function of pressure and temperature. Combustion product omissions and G-W reactivity are based on in-house experimental testing, proprietary communications, and a US Army report <sup>9,14</sup>. The CCET code assumes that as the gas diffuses to the wall, it reacts to form products as follows:

$$B_a = (C_w - C_{cg})/C_g \quad (1)$$

where  $C_w$  is the mass fraction of wall material and  $C_g$  is the mass fraction of the gas edge <sup>9</sup>.

The MABL code <sup>6,9</sup> outputs adiabatic wall recovery enthalpy ( $H_r$ ) and adiabatic wall temperature ( $T_{aw}$ ) data as a function of time and travel. The recovery enthalpy is the potential chemistry driver where the heat transfer approaches zero and the adiabatic wall temperature is the potential temperature without reactions. The MABL code also outputs cold wall heat transfer rate ( $Q_{cw}$ ) data as a function of time and travel. This heat transfer rate is the wall heat flux evaluated at the cold wall temperature. The MABL code heat and mass transfer model includes the following three equations. The first equation for mass addition to the boundary layer, the second equation for heat-to-mass transfer ratio, and the third equation for

the overall correlation between the first and second equations:

$$r_e U_e Ch_o = Q_{cw}/(H_r - H_{gw}) \quad (2)$$

$$r_e U_e Ch_b = Mdot_g/B_a; Le = 1 \quad (3)$$

$$Ch_b/Ch_o = f(B_a, M_w) = 1 - (h Mdot_g/r_e U_e Ch_o) \quad (4)$$

where  $r_e$  is edge density,  $U_e$  is edge velocity,  $Ch_o$  is Stanton # without blowing,  $Q_{cw}$  is cold wall heat transfer,  $H_r$  is recovery enthalpy,  $H_{gw}$  is G-W enthalpy,  $Ch_b$  is Stanton # with blowing,  $Mdot_g$  is gas mass transfer,  $Le$  is Lewis number,  $B_a$  is ablation potential,  $M_w$  is molecular weight, and  $h$  is  $f$ (G-BL molecular diffusion) <sup>9</sup>.

The MACE code <sup>7,9</sup> calculates the actual transient thermochemical response and generates wall material erosion predictions and comparisons (ablation, conduction, and erosion profiles) as a function of time, travel (customer selected 6", 12", 30"), and number of rounds to barrel condemnation. The nitrided A723 and 0.002" plated Cr/A723 wall materials are evaluated for maximum wall temperature and erosion using the M242 Cycle A firing scenario. The MACE code can do any propellant-gun barrel combination on a high end PC; Each mechanism's importance is identified and incremental upgrades are feasible.

The M242/M791 MACE maximum wall temperature gun system predictions are compared to those of the US Army's standard gun barrel finite difference heat transfer code (FDHEAT) <sup>16</sup> that calculates the transient temperature distribution in a multilayered cylinder and models radial/axial heat flow separately. The nitrided A723 and 0.002" plated Cr/A723 wall materials are evaluated by FDHEAT for maximum wall temperature using the M242 Cycle A firing scenario. The M242/M791 gun system predictions are also compared to actual M242/M791 nitrided A723 experimentally measured gun system erosion data.

### RESULTS AND DISCUSSION

Figure 1 provides a gun erosion modeling overview that includes the bore surface erosion analysis using the ABAQUS, XNOVAKTC, CCET, MABL, and MACE codes. In addition, this Figure provides an

overview of the subsurface erosion analysis using metallographic data and the XNOVAKTC, CCET, MABL, and MACE codes.

Figure 2 gives the calculated ambient temperature conditioned 25mm M242/M791 XKTC data for: gas velocities (V), gas temperatures (T), and gas pressures (P) as a function of time for the 6", 12", and 30" RFT customer selected axial positions.

Figure 3 gives the calculated ambient temperature conditioned 25mm M242/M791 MABL data for: recovery enthalpies (Hr) and cold wall heats (Qcw) as a function of time for the same customer selected axial positions above. The data in Figure 3 are two of three parts of the driving potential (Qcw / (Hr-Hgw)) which is essentially mass affected per unit area per unit time.

Figure 4 gives the calculated 25mm M242/M791 CCET data for: reacting wall enthalpies (Hw) and ablation and melting potential (Ba) for HC Cr and nitrided A723 as a function of temperature. This data in the left plot of Figure 4 is the third of three parts of the driving potential (Qcw / (Hr-Hgw)) which again is essentially mass affected per unit area per unit time. For HC Cr metal, Figure 4 shows that it oxidizes at 3600 R (3110 F), it melts at 3830 R (3340 F), and its oxide melts at 4570 R (4080 F). For nitrided A723 steel, Figure 4 shows that it oxidizes at 1900 R (1410 F), its oxide melts at 2960 R (2460 F), and it melts at 3250 R (2760 F). The nitrided A723 wall oxidizes substantially below its metallic melting point while the HC Cr wall oxidizes just below its metallic melting point. The nitrided A723 wall has an expansive flaking oxide which enhances further oxidation while the HC Cr wall has a passivating oxide which prevents further oxidation. The nitrided A723 wall oxide melts well below its metal while the HC Cr wall oxide melts well above HC Cr metal.

Figure 5 shows the calculated 25mm M242/M791 MACE surface/subsurface exposure and flow modeling for the 6" RFT axial position. The upper part of this Figure shows the first 0.002" nitrided A723 steel with 100% of the A723 surface exposed for thermochemical ablation. The lower part of this Figure shows the 0.002" HC Cr plate over the first 0.002" A723 with its 0.0070" average HC Cr plates and 0.0005" average crack widths. For the last 90% of the gun's life, 12% of the A723 subsurface is

exposed for thermochemical ablation. When a pair of 0.0035" wide average A723 voids occur below adjacent HC Cr crack bases, metallography and modeling tell us that the 0.0070" Cr plate spalls and it should be noted that about half the area under the plate is consumed. Variation of exposed area of subsurface A723 varies its Qint, Tint, and driving potential (Q / dH). Cyclic thermal induced evolution of mainly H<sub>2</sub>O, O<sub>2</sub>, H<sub>2</sub>, and Cl<sub>2</sub> gives HC Cr shrinkage and heat check cracking. HC Cr achieves "maximum" shrinkage/cracking at ~10% of the gun's life for M791 rounds using the Cycle A firing Scenario. A723 thermochemical gas wash at heat checked crack bases and after platelet spalling enhance mechanical pitting and chipping.

Figure 6 gives the MACE calculated ambient temperature conditioned 25mm M242/M791 maximum wall and interface temperatures as a function of rounds for the 150 round Cycle A and single shot firing scenarios. In order of decreasing maximum wall and interface temperature, the six curves given in this figure are for: bare A723 steel after the Cycle A firing scenario (CA), HC Cr plate after the Cycle A firing scenario, the Cr/A723 interface after the Cycle A firing scenario, bare A723 steel after a single shot scenario (SS), HC Cr plate after a single shot scenario, and the Cr/A723 interface after a single shot scenario. The highly verified FDHEAT code<sup>16</sup> is considered the US Army ARDEC standard code for wall temperature predictions and all respective MACE data is within 100 degrees F of the corresponding FDHEAT data.

In Figure 6, the iron oxide melting point (MP), A723 melting point, HC Cr temperature of reaction (Tr), HC Cr melting point, and chromium oxide melting point are all above 2400 degrees F and do not pertain to the presented data. HC Cr is thermochemically inert at the 6", 12", and 30" RFT positions for both the Cycle A and single shot firing scenarios. Bare A723 steel and the Cr/A723 interface are thermochemically reactive at the 6", 12", and 30" RFT positions for Cycle A firing scenario since they exceed the A723 temperature of reaction. Bare A723 steel is thermochemically reactive at the 6" and 12" RFT positions, thermochemically inert at the 30" RFT position for the single shot firing scenario since only the first two positions exceed the A723 temperature of reaction. The Cr/A723 interface is thermochemically inert at the 6", 12", and 30" RFT positions for the single shot firing scenario since none of these positions exceed the A723 temperature of reaction.

Figure 7 gives the MACE calculated ambient temperature conditioned 25mm M242/M791 cumulative wall erosion to condemnation as a function of M791 rounds. As highlighted, the 25mm M242 gun erosion condemnation is when A723 gas wash first exceeds 0.020" at any location. Also highlighted, A723 gas wash onset is at 0.002" and as the interface degrades then the Cr plate begins spalling platelets forming pits.

In Figure 7, the left-most of the two curves is for the typical M791 6" RFT nitrided A723 which achieves erosion condemnation at 4000 rounds and this agrees to within 10% of the number of rounds given in the M242/M791 gun system technical data package <sup>12</sup>.

In the gun life, nitrided A723 is uneroded at the 12" and 30" RFT positions. The right-most of the two curves is for the typical M791 6" RFT HC Cr plated A723 which achieves A723 gas wash onset at 4200 rounds and erosion condemnation at 8200 rounds. If HC Cr chips, A723 erosion begins at that round number. In the gun life, HC Cr is uneroded at the 6", 12" and 30" RFT positions and the A723 interface is uneroded at the 12" and 30" RFT positions despite HC Cr chipping.

#### REFERENCES

1. von Karman, T., Sorbonne Lectures, 1951-1952; see also Princeton University Lectures, 1953; "Fundamental Approach to Laminar Flame Propagation," AGARD Selected Combustion Problems, Butterworths, London, 1954; and "Fundamental Equations in Aerothermochemistry," Proc. 2nd AGARD Combust. Colloq., Liege, Belgium, 1955.
2. Reshotko, E., and Cohen, C.B., "Heat Transfer at the Stagnation Point of Blunt Bodies," NACA TN Number 3513, July 1955.
3. Cohen, C.B., Bromberg, R., and Lipkis, R.P., "Boundary Layers with Chemical Reactions Due to Mass Additions," Report No. GM-TR-268, The Ramo-Wooldridge Corporation, Los Angeles, CA, 1957.
4. Denison, M.R., and Dooley, D.A., "Combustion in the Laminar Boundary Layer of Chemically Active Sublimators," Publication No. C-110, Aeronutronic Systems, Inc., Glendale, CA, 1957.
5. Lees, L., "Convective Heat Transfer with Mass Addition and Chemical Reactions," Combustion and Propulsion, Proc. 3rd AGARD Combust. Colloq., Palermo, Sicily, Pergamon Press, NY, 1958; see also Recent Advances in Heat and Mass Transfer, McGraw-Hill, New York, 1961.
6. Nickerson, G., Berker, D., Coats, D., and Dunn, S., "Two-Dimensional Kinetics (TDK) Nozzle Performance Computer Program," Software and Engineering Associates, Inc., Carson City, NV, 1993.
7. Dunn, S., "Materials Ablation Conduction Erosion Program (MACE)," Software and Engineering Associates, Inc., Carson City, Nevada, 1989.
8. Gordon, S., and McBride, B., "Computer Program for Calculation of Complex Chemical Equilibrium Compositions, Rocket Performance, Incident and Reflected Shocks, and Chapman-Jouguet Detonations (CET)," NASA SP-273, NASA Lewis Research Center, Cleveland, OH, 1971.
9. Dunn, S., Sopok, S., "Modification Of The TDK/MACE Rocket Erosion Code To The Gun Barrel Erosion Code"; Also "Workshop On Gun Barrel Erosion", Software & Engineering Associates, Carson City, NV, US Army Benet Labs, Watervliet, NY, 1992-1993.
10. Freedman, E., "BLAKE - A Thermodynamic Code Based on Tiger: User's Guide and Manual," US Army Ballistic Research Laboratory Technical Report, Aberdeen Proving Ground, MD, 1982.
11. Gough, P., "The XNOVAKTC Code," Paul Gough Associates, Portsmouth, NH, 1990.
12. 25-mm M242/M791 Bushmaster Gun System Technical Data Package, US Army ARDEC, Dover, NJ, 1990 - 1993.
13. Picard, J., Ahmad, I., and Bracuti, A., Proceedings of the Tri-Service Gun Tube Wear and Erosion Symposiums, US Army ARDEC/ADPA, Dover, NJ, 1970, 1972, 1977, and 1982.
14. Alkidas, A., Morris, S., Christoe, C., Caveny, L., and Summerfield, M., "Erosive Effects of Various Pure and Combustion-Generated Gases on Metals - Part II," US Army Materials and Mechanics Research Center Technical Report, Watertown, MA, 1977; see also Part I, 1975.
15. Dunn, S., Sopok, S., Coats, D., O'Hara, P., Nickerson, G., and Pflegl, G., "Unified Computer Model For Predicting Thermochemical Erosion In Gun Barrels," Proceedings of 31st AIAA Propulsion Meeting, San Diego, CA, July, 1995.
16. Witherell, M., "FDHEAT Gun Barrel Heat Transfer Code", US Army Benet Labs, Watervliet, NY, 1992-1996.

Figure 1 - Gun Erosion Modeling Overview

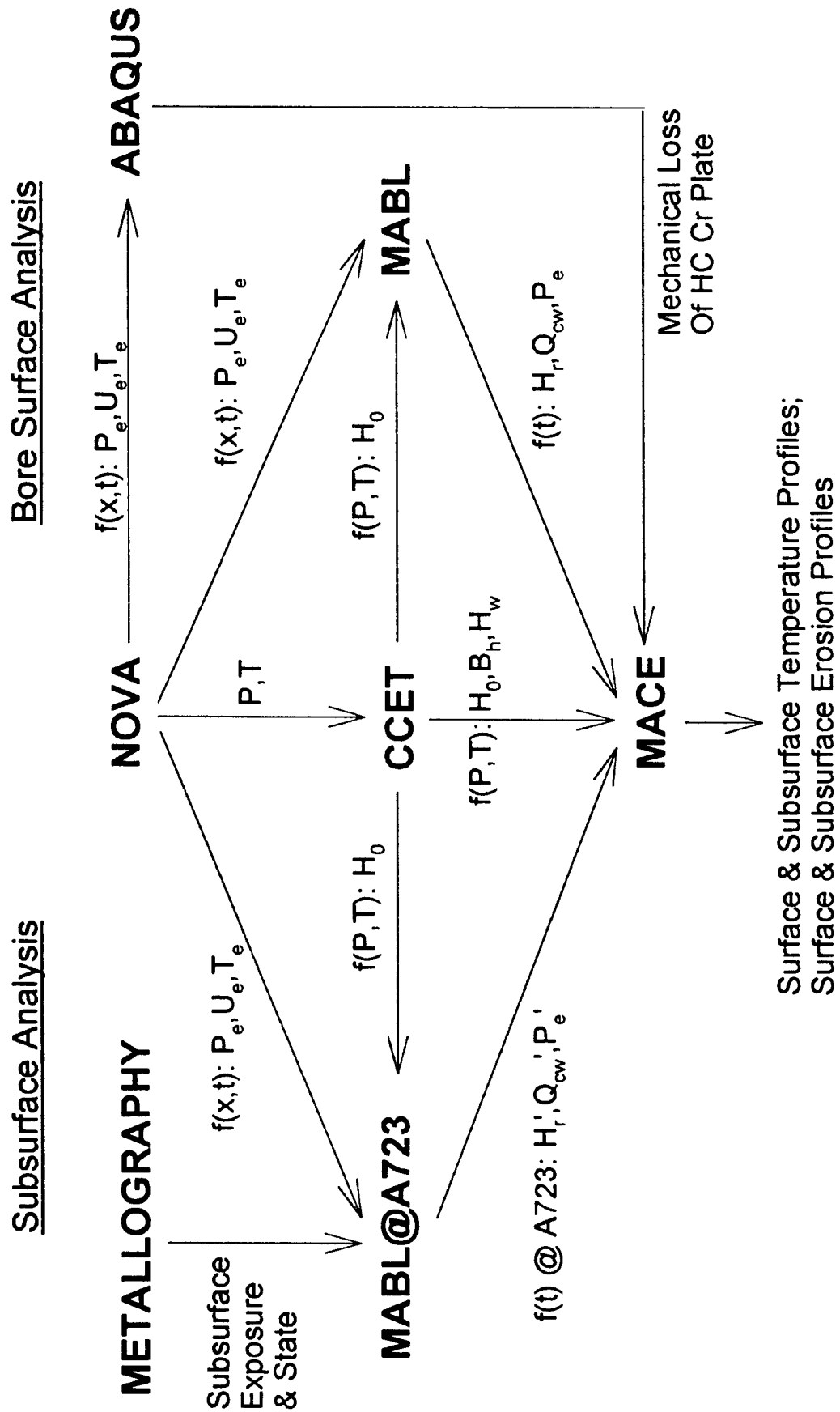


Figure 2 - Ambient Conditioned 25mm M242/M791 XKTC Data

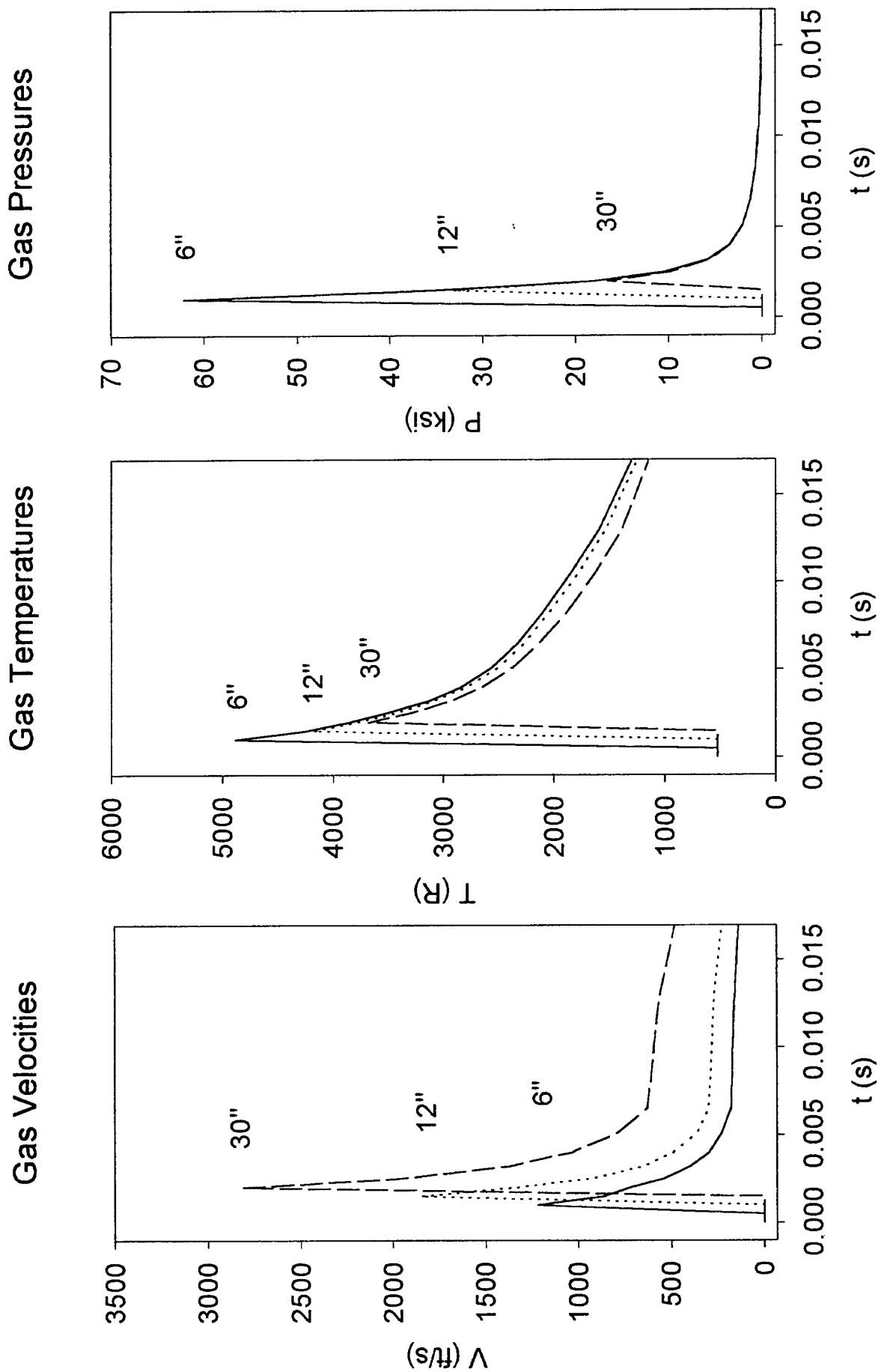
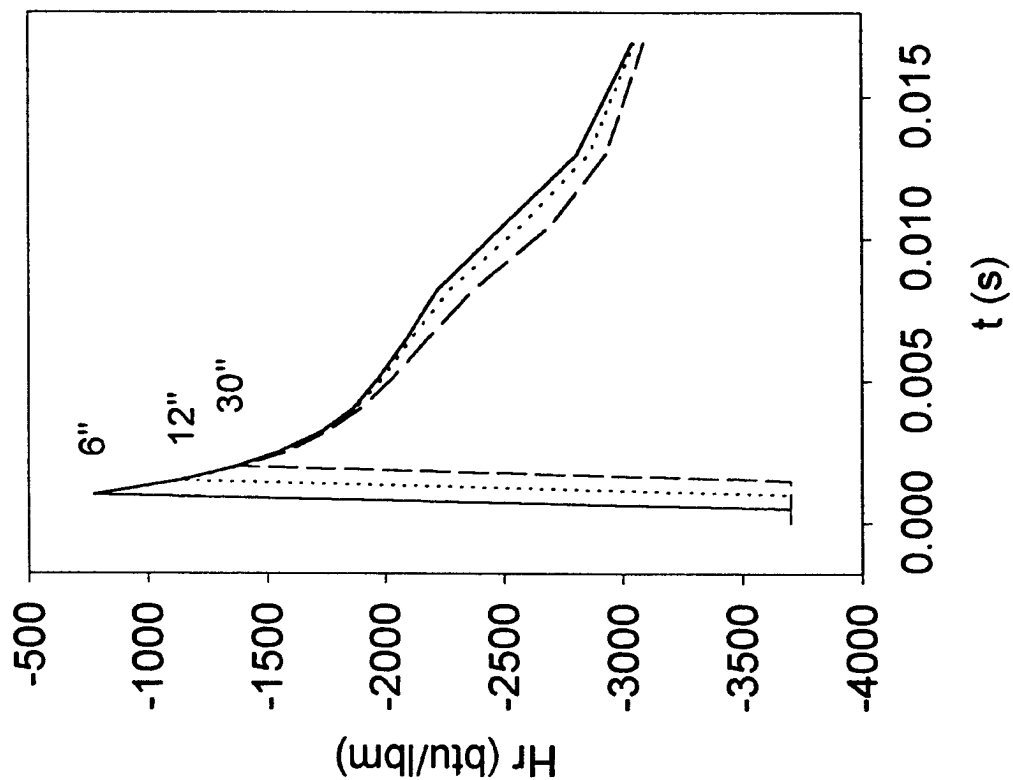


Figure 3 - Ambient Conditioned 25mm M242/M791 MABL Data

( $Q_{cw} / (Hr-Hgw) = \text{Mass Affected} / \text{Area Time} = \text{Driving Potential}$ )

### Recovery Enthalpies



### Cold Wall Heats

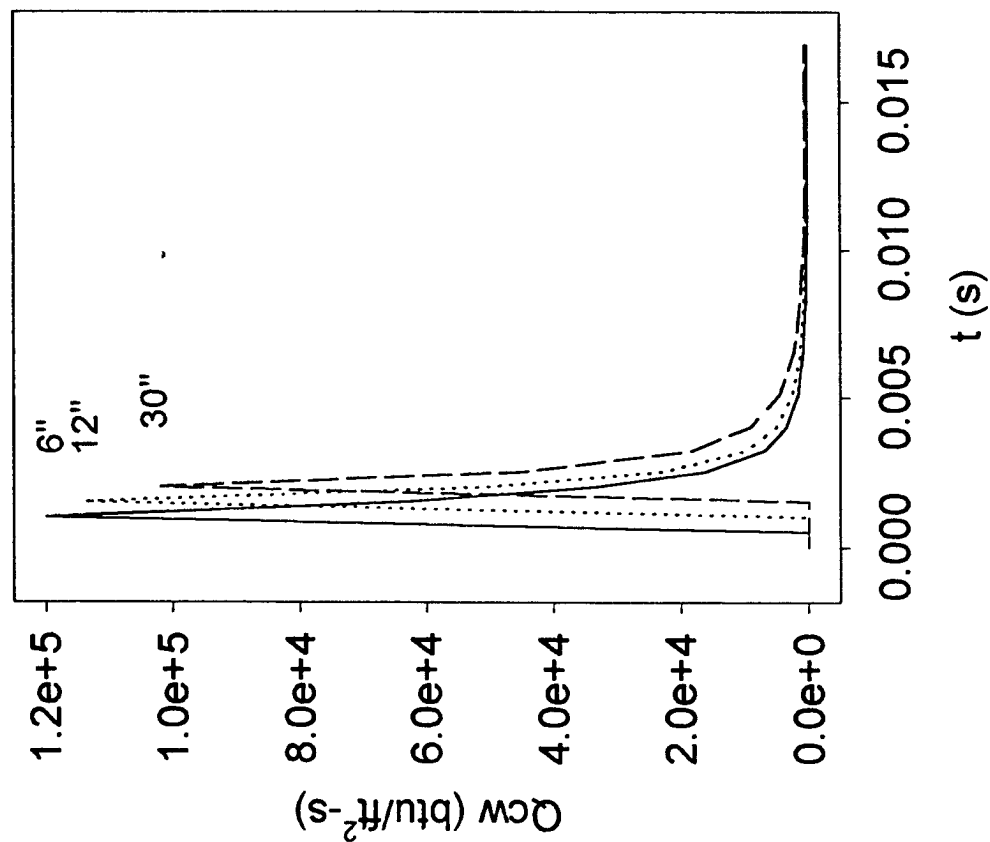


Figure 4 - 25mm M242/M791 CCET Data

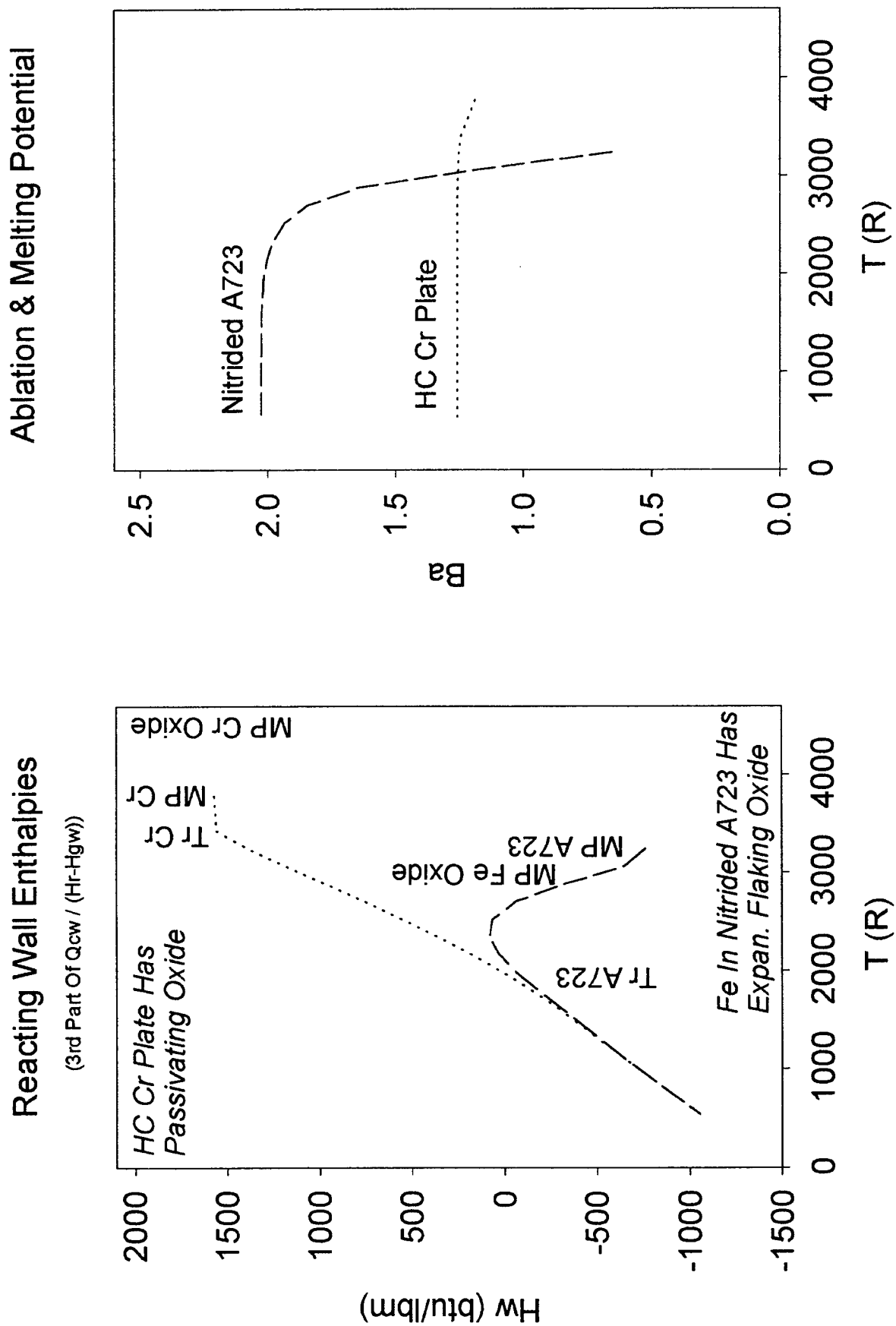


Figure 5 - 25mm M242/M791 6" RFT Surface/Subsurface Exposure & Flow Modeling

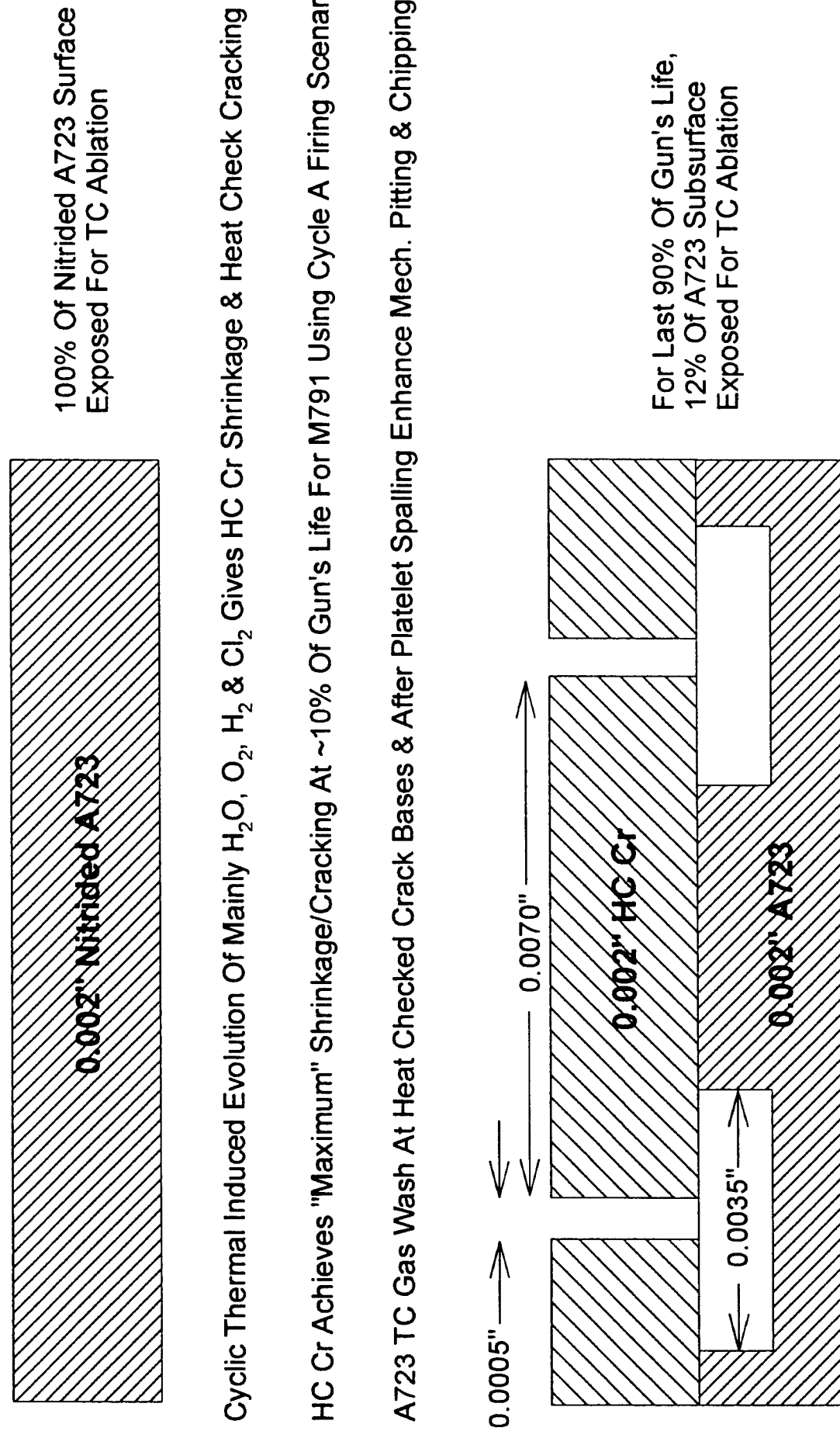


Fig. 6 - MACE Ambient Cond. 25mm M242/M791 Max. Wall & Interface Temperatures

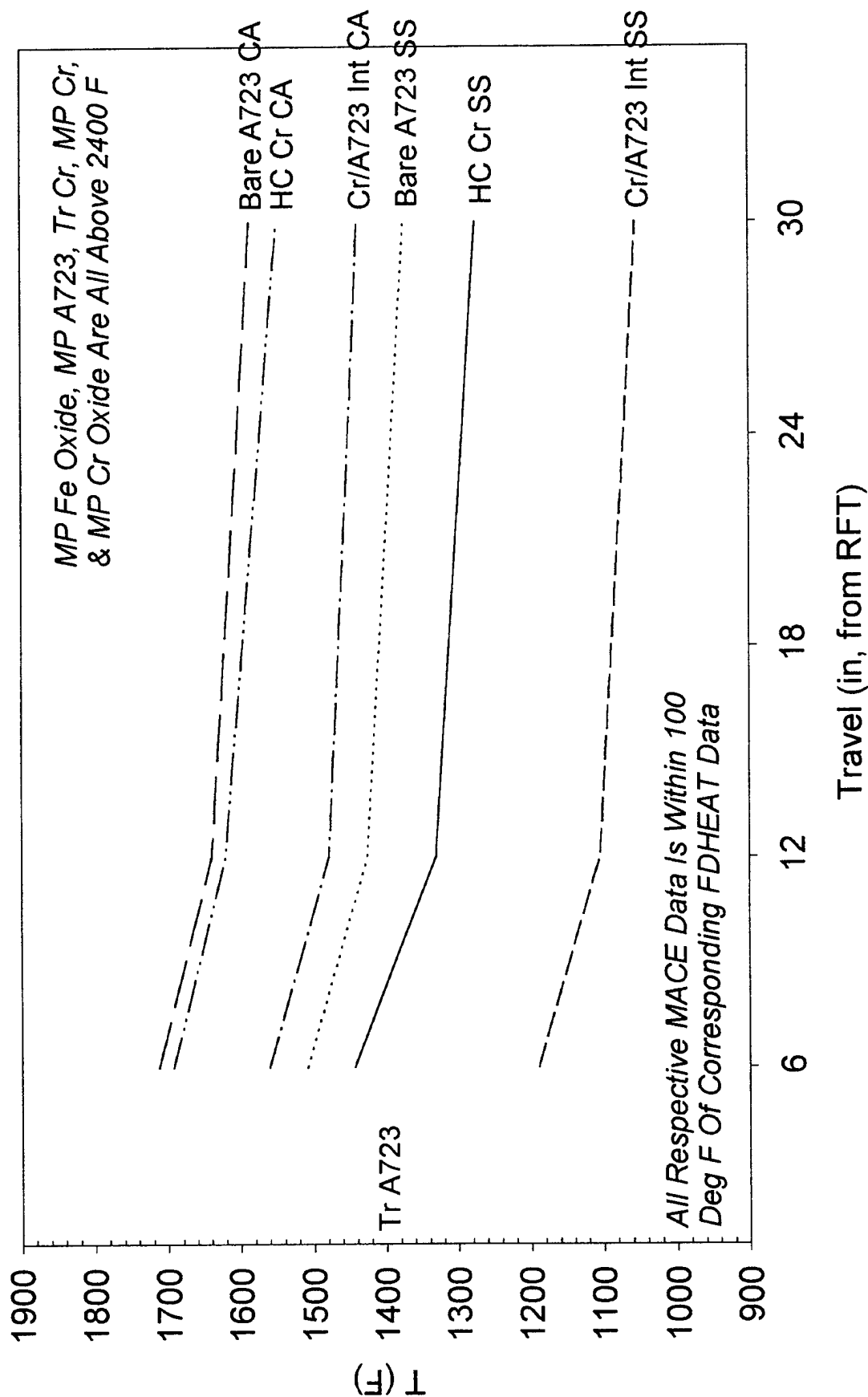


Fig. 7 - MACE Ambient. Cond. 25mm M242/M791 Cum. Wall Erosion To Condemnation

